partitioning in the case of this relatively small hydrophilic monocation compared to the distinct binding observed with the larger, more hydrophobic CBP^+ underlines the role of hydrophobic factors and once again reinforces the idea that these cations as well as probably many other polar organic molecules are solubilized or interact with micelles by binding at hydrophobic-hydrophilic interfaces.

Acknowledgment. We are grateful to the National Science Foundation (Grant No. CHE 7823126) for support of this work.

Catalytic Water Reduction at Colloidal Metal "Microelectrodes". 2. Theory and Experiment

Deborah S. Miller,[†] Allen J. Bard,[‡] George McLendon,*[†] and J. Ferguson[†]

Contribution from the Departments of Chemistry, University of Rochester, Rochester, New York 14627, University of Texas at Austin, Austin, Texas 78712.
Received October 6, 1980

Abstract: A simple theory based on electrochemical principles is presented which predicts some of the catalytic properties of the widely used colloidal metal dispersions. The theory has been specifically applied to the case of photocatalytic water reduction to H_2. The model assumes that the kinetic properties of the system are governed by the current-potential curves of the half-reactions and that the reaction velocity can be determined by finding the common potential at which the current attributable to the mediator (e.g., methyl viologen) oxidation is equal to that for proton reduction at the metal surface. The effects of pH, mediator potential, and colloid size and composition can be predicted. These predictions have been experimentally verified with methyl viologen radical cation generated electrochemically and photochemically (via the $Ru(bpy)_3^{2+}$-*N*-phenylglycine system) and with other mediators at colloidal dispersions of several metals.

The catalytic reactions of metal colloids have been the subject of long and fruitful study.[1-6] Interest in these systems has been further increased by their use as necessary cocatalysts in photocatalytic water reduction schemes.[7-9] This latter use has prompted preliminary investigations of the mechanisms by which these metal particles facilitate water reduction by a reduced mediator, like methyl viologen radical cation ($MV^{+\cdot}$). Analogy suggests that these colloids may act as "microelectrodes", with a potential determined by the photoreduced mediator.[2,4,8] Using this analogy, several groups have quite recently presented kinetic studies of methyl viologen dependent H_2 production at dispersed Pt, Au, and other metals.[2,4,10,11] Grätzel has reported some empirical determinants of colloidal catalyst efficiency, including the effects of colloid size and protective agents. Limiting rates for the catalyst reaction with $MV^{+\cdot}$ were also reported.[4] More mechanistic approaches have been taken by other groups. Kopple et al. have reported isotope effect studies of H_2 production on Au colloids.[2] The observed isotope effects are quite similar to those observed at bulk electrodes, supporting the microelectrode analogy. Miller and McLendon have reported extensive rate studies of colloidal catalysis of water reduction with different metals and varying mediator potential.[10] In the studies of Meisel and Heinglein,[3] the observed rate data were treated with the use of microscopic kinetic models. While this approach is interesting, it suffers from a limited ability to predict quantitatively the effects of reaction variables on catalytic efficiency. To date, no such predictive theory is available for the important catalytic water reduction reaction, nor are sufficient experimental results available for a definitive test of any theory.

The suggestion that heterogeneous catalysis of electron transfer reactions at metals or carbon can be interpreted in terms of the electrochemical behavior of the reactants involved in the process has been discussed previously,[6,12] based on a model first proposed for corrosion reactions.[13] Most recently Spiro[12] has discussed the special cases of (a) two totally irreversible reactions in the absence of mass transfer effects and (b) a totally irreversible reaction coupled with a mass transfer limited one in the limiting current regime. General models have apparently not been proposed, however, nor have attempts been made to use these in a more predictive way in homogeneous photocatalytic processes involving heterogeneous catalysts. In the present manuscript, a general model is proposed and quantitatively extended which predicts a wide variety of experimental data for colloidal catalysis of water reduction. It is the purpose of this manuscript to present explicitly this predictive model for colloidal catalysis in the hydrogen evolution reaction. In this model, the colloidal "microelectrode", like a bulk electrode, serves several functions. It provides a medium by which the number of electrons (or equivalents) of the two half-reactions can be matched. It also provides a surface for lowering the activation energy of one or both of the half-reaction processes. In the process under consideration here, the one-electron oxidation of the donor $MV^{+\cdot}$ is matched to the overall two-electron process producing H_2. Moreover, the adsorption of hydrogen atoms on the surface of the metal lowers the energy required for the reduction step H^+

[†] University of Rochester.
[‡] University of Texas at Austin.

(1) W. P. Dunworth and F. F. Nord, *Adv. Catal.*, **6**, 125-141 (1954).
(2) K. Kopple, D. Meyerstein, and D. Meisel, *J. Phys. Chem.*, **84**, 870-875 (1980).
(3) A. Henglein, *J. Phys. Chem.*, **83**, 2209-2216 (1979).
(4) J. Kiwi and M. Gratzel, *J. Am. Chem. Soc.*, **101**, 7214-7217 (1979).
(5) J. Turkevich, P. C. Stevenson, and J. Hillier, *J. Discuss, Faraday Soc.*, **11**, 55-75 (1951).
(6) M. Spiro and A. B. Ravno, *J. Chem. Soc.*, 78-96 (1965).
(7) J. M. Lehn and J. P. Sauvage, *Nouv. J. Chim.*, **1**, 449 (1977).
(8) K. Kalyanasundaram, J. Kiwi, and M. Gratzel, *Helv. Chim. Acta*, **61**, 2720 (1978).
(9) A. Moradpour, E. Amouyal, R. Keller, and H. Kagan *Nouv. J. Chim.*, **2**, 547 (1978).
(10) (a) D. S. Miller and G. McLendon, *Inorg. Chem.*, **20**, 950-953 (1981). (b) In principle, the ratio of $MV^{+\cdot}/MV^{2+}$ may change in the course of catalysis so that the position of the anodic curve would shift rather than remaining fixed in Figure 1. In practice, this shift is small under the (common) experimental conditions reported here; the total shift of $pH_{1/2}$ due to the changing ratio of $MV^{+\cdot}/MV^{2+}$ is <0.1 pH unit.
(11) G. Frens, *Natl. Phys. Sci.*, **241**, 20 (1973).
(12) M. Spiro, *J. Chem. Soc., Faraday Trans. 1*, **75**, 1507-1512 (1979), and references therein.
(13) C. Wagner and W. Traud, *Z. Elektrochem.*, **44**, 391 (1938).

0002-7863/81/1503-5336$01.25/0

+ e → H· compared to that in homogeneous solution. The resulting reaction rate can be predicted from the individual current–potential curves of each couple, as explained below. The predictive model is tested by experimental results on hydrogen production at metal colloids by using a photocatalytic or novel electrogenerated mediator experimental approach. Properties of specific interest include the effects on catalytic efficiency of pH, mediator potential, and colloid composition (both elemental composition and size).

Experimental

Materials. The poly(vinyl alcohol) stabilized platinum colloid was prepared following the method of Kiwi and Grätzel.[4] Poly(vinyl alcohol) (Aldrich, 100% hydrolyzed, average mol wt = 86 000) and K_2PtCl_6 (Alfa) were used without further purification. After preparation, the colloid solution was centrifuged at 12 000 rpm at 20 °C for 2 h. The transparent yellow supernatant solution was used in the water reduction experiments.

Au citrate colloids were prepared by the methods of Frens from $HAuCl_4$ (Aldrich) and sodium citrate (Merck).[11] Ag colloids and finely divided Ni were prepared as previously described.[27] $DMPB^{2+}$ (4,4′-dimethyl-1,1′-propylene-2,2′-bipyridine dibromide) was prepared and its reduction potential determined as previously described by Miller and McLendon.[10]

Other materials were reagent grade and used without further purification: methyl viologen (Aldrich); tris(bipyridyl)ruthenium dichloride (G.F. Smith); EDTA (Sigma); and *N*-phenylglycine (Aldrich).

Methods. H_2 Production with Electrogenerated Mediator. This procedure involved electrolytically reducing the mediator (med^{2+}) to produce the radical cation ($med^{+}\cdot$) which reduces water to H_2 in the presence of a colloidal metal catalyst. Deaerated buffered solutions (pH 3.0–5.8: 0.05 M phthalate/0.1 M KNO_3; pH 5.8–7.0: 0.05 M phosphate/0.1 M KNO_3) containing 2×10^{-3} M mediator and centrifuged Pt catalyst (approximate concentration 10^{-6} M Pt) were electrolyzed at −1.0 V (vs. SCE) in a specially designed gas-tight electrochemical cell. Appropriate controls showed no H_2 was produced in the absence of MV^{2+}. Trace H_2 was produced in the (apparent) absence of Pt. A Hg pool working electrode, an isolated Pt gauze axiliary electrode, and a saturated calomel reference electrode were used. The N_2 atmosphere above the solution was frequently sampled and H_2 measured by gas chromatography (43 °C, Porapak Q column, N_2 carrier gas). The solution pH was checked before and after electrolysis. Hydrogen production was corrected for background current and for trace amounts of H_2 produced in the absence of Pt at lower pH.

Photocatalytic H_2 Production. The photocatalytic experiments were based on a standard model system[7-10] for water photoreduction as described in detail elsewhere.[10] $Ru(bpy)_3^{2+}$ (10^{-5} M) was used as the photocatalyst, methyl viologen (10^{-3} M) as the electron transfer quencher, *N*-phenylglycine as the ultimate electron donor, and a colloidal metal ($\sim 10^{-6}$ M), prepared as described above. *N*-Phenylglycine was chosen as the electron donor since, unlike EDTA, it can be efficiently oxidized at low pH. The solutions were irradiated with a 350 W tungsten–halogen lamp. The light was filtered to provide irradiation only between 400 and 500 nm. Lamp intensity was monitored by actinometry with Reinecke's salt.[14] The H_2 produced was monitored by gas chromatography as above.

Results and Discussion

Theory. Let us consider the major features of the electrochemical model for catalysis. Since the colloid microelectrode functions in the same manner as a bulk electrode, the individual current–potential (i–E) curves for both half-reactions hold, as shown in a simplified representation[10b] in Figure 1; the more general case is shown in Figure 6. At a steady state the individual anodic and cathodic currents (i.e., the net oxidation and reduction rates at the surface) must be equal. Thus the particle attains a mixed potential, E_m, at which the rate of reaction is v_m and the partial currents are i_m. This overall process can thus be considered as a means of matching the donor and acceptor redox potentials and electron transfer rates.

This concept of employing i–E curves to model heterogeneous processes dates from the classical work by Wagner and Traud[13] on corrosion. In addition to previous studies of heterogeneous redox catalysis,[6,12] such models have also been employed to explain

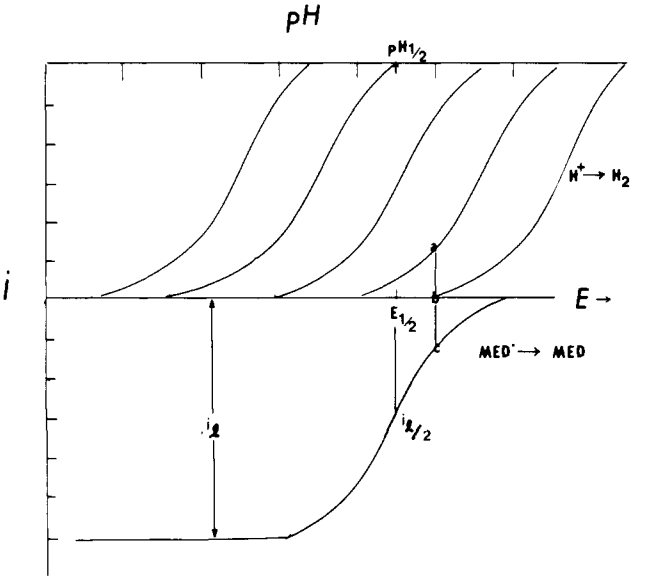

Figure 1. Current–voltage curves for the potential matching of an anodic reaction (mediator$^{+}\cdot$ → mediator) with a cathodic reaction ($H^+ \rightarrow {}^1/_2H_2$). The current, or rate of H_2 formation, at each pH is predicted by the vertical displacement between the zero current line and the anodic (mediator) curve (line bc). At low pH, the rate i_{1H2} is assumed to be limited by mediator mass transport. The rate at half maximal velocity $i_{1/2}$ defines the "Nernst" potential for the hydrogen reaction ($E_{1/2}$ or $pH_{1/2}$).

heterogeneous photocatalysis at semiconductor powders.[15-17] A detailed general mathematical model is described in Appendix I. Applications to the particular case of the mediated H_2 production reaction are described below.

pH Effects. Several predictions immediately arise from this representation. First, the current, or rate of H_2 production, will depend on the pH of the solution (and on the reduction potential of the mediator). For the mediated H_2 evolution reaction of interest here, the oxidation of the donor (e.g., $MV^{+}\cdot$) is rapid and occurs in a nerstian reaction at the electrode. At a given $[med^{+}\cdot]/[med^{2+}]$ ratio and mass transfer rate, the anodic i–E curve will remain fixed and be independent of pH (see Appendix IC and Figure 1). The cathodic current for proton reduction is pH dependent, however. The observed rate at a given pH can be found by considering both i–E curves simultaneously. For example, at the pH labeled "a" in Figure 1, the rate of H_2 production is predicted by line bc. This line extends to intersect the family of cathodic water reduction curves. At a given pH, the reduction rate must equal the oxidation rate, and one cathodic wave, determined by the pH-dependent overpotential, will be intersected such that ab equals bc. A convenient reference point in treating the effect of pH on the catalytic reaction is that pH at which the $i_m = ({}^1/_2)i_l$, called $pH_{1/2}$, which occurs at

$$E_m = E(\text{med}) = E^0(\text{med}) - (RT/nF) \ln (C_Q^*/C_R^*) \quad (1)$$

(where i_l is the mass transport limited current for mediator oxidation) (see Appendix). For the $MV^{2+}/MV^{+}\cdot$ system, $E_m = -0.44$ V vs. NHE at $pH_{1/2}$. The value of i_m at this pH depends upon the kinetics of the hydrogen evolution reaction (h.e.r). As shown in the Appendix, the determination of $pH_{1/2}$ may be useful in extracting the rate constant for this reaction; see eq A24.

At higher pHs the i_m value approaches zero since the cathodic i–E curve shifts to more negative values as the pH increases. If the h.e.r. follows the totally irreversible path implied by eq A23, then the cathodic i–E curve will shift ~120 mV toward more negative potentials for each unit increase in pH. At lower pH the rate of H_2 production will increase sharply, and i_m ultimately

(14) E. E. Wegner and A. W. Adamson *J. Am. Chem. Soc.*, **88**, 394 (1966).

(15) A. J. Bard, *J. Photochem.*, **10**, 59–75 (1979).
(16) A. J. Bard, *Science (Washington, D.C.)*, **207**, 139–144 (1980).
(17) B. Kraeutler and A. J. Bard, *J. Am. Chem. Soc.*, **100**, 2239–2240 (1978).

reaches the limit i_l, set by the mass transport of the reduced mediator to the colloid surface. Beyond this point, any further pH decrease cannot increase the rate.

The pH at which mediator mass transport becomes rate limiting will clearly depend on mediator concentration (see, e.g., equation A24 in the Appendix).

For example, at $[MV^{+}\cdot] = 10^{-3}$ M, $pH_{1/2} = 6.3$, but at $[MV^{+}\cdot] = 10^{-2}$ M, $pH_{1/2} \simeq 5.3$, and the mass transport limit would be hard to observe. (The mass transport limit will lie ca. 0.06 (1 pH unit) below $pH_{1/2}$).

Metal Effects. Just as bulk metal electrodes exhibit different rate constants for the h.e.r., i.e., different hydrogen overpotentials, so should potentiated colloids of different metals exhibit different catalytic efficiency. In the present model, the effect of an overpotential for H_2 production at a given metal will be to shift the pH curves along the potential axis. As the h.e.r. rate constant decreases, the overpotential increases, so that a shift to lower pH will be required to maintain the same net driving force and thus to maintain the same rate. According to eq A24, each tenfold decrease in k_1^0 (~120 mV increase in overpotential) must be compensated by a unit decrease in pH to maintain i_m constant. By going to sufficiently low pH, it therefore should be possible to produce H_2 at the mass transfer limited rate, even for metals with considerable hydrogen overpotentials (e.g., Ni or Ag). Thus, under these conditions, a relatively inexpensive metal could be substituted for Pt with no decrease in catalytic efficiency. The effect of colloid size on the rate of electrode reactions also can be simply predicted. Since the total current is proportional to area, the rate of H_2 production should increase linearly with colloid area. For spherical particles, the area will scale as $1/r$, the ratio of area/volume, assuming a constant total amount of metal.

Mediator Effects. In like manner, the effect of using homologous mediators with different standard potentials can be predicted easily. A change in mediator potential will shift the anodic (mediator) curve along the potential axis. More strongly reducing mediators will allow H_2 production at a higher pH than mediators with lower potentials. The quantitative effect of this shift on rate (relative to the mass transfer limit) under the conditions of eq A23 is roughly a 0.12 V shift in E_m^0 being equivalent to a unit pH change.

Thus, this simple model makes a number of testable predictions about the effect of experimental variables on the electron transfer reactions of metal colloids. In the following section a series of experiments designed to test these predictions is described.

Results and Discussion

pH variation. As discussed above, the electrochemical model predicts a rapid change in rate around the pH where the i–E curves for H^+ reduction and mediator oxidation match (i.e., $E_m = E_{1/2}(\text{med})$, $pH = pH_{1/2}$). Above this pH, the rate of H_2 evolution will rapidly fall to zero. Below this pH, the rate will rise, but is predicted to reach a limit set by mediator mass transport. Beyond this point, increased acidity should not increase the rate. The change in $[med^{2+}]/[med^{+}\cdot]$ with pH was not sufficient to significantly shift the anodic mediator i–E curve.) These predictions are confirmed by the results presented in Figures 2 and 3. Effective $pH_{1/2}$ values, which include the effect of metal overpotential, are indicated in each figure. Figure 2 presents results for photocatalytic H_2 generation. The results in Figure 3 were obtained in an electrogenerated mediator experiment. Details of the experiments are contained in the methods section. Importantly, both systems show essentially the same pH dependence. The excellent correspondence between the simple electrogeneration experiments in which only $MV^{+}\cdot$ and Pt are present and the potentially more complex photocatalytic experiments demonstrates that H_2 production in the photocatalytic system is controlled by the heterogeneous catalytic step. Under the present conditions, in which the competing rates of amine oxidation and back reaction remain constant, the rate of H_2 formation is ultimately governed by the reaction chemistry at the metal colloid.

A quantitative test of theory is shown in Figure 3, in which the predicted dependence of hydrogen production rate, expressed as

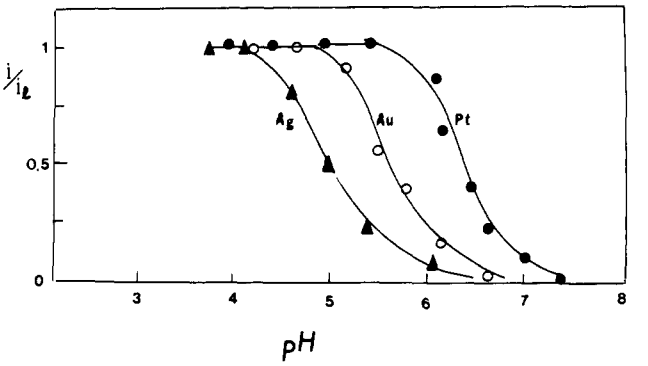

Figure 2. Rate of H2 production as a function of pH in a photocatalytic system (see methods for details). (The system includes a methyl viologen mediator, *N*-phenylglycine electron donor, and $Ru(bpy)_3^{2+}$, as the photoacceptor.) Results are normalized relative to maximum rate (i_l) to allow ready comparison of data for Pt (●), Au (○), and Ag (△) colloids.

i/i_l vs. pH for reasonable values of the parameters, follows the experimental data quite closely. For the approximate conditions of the experiment in Figure 3, $pH_{1/2} = 6.3$, yielding a rate constant for the h.e.r., k_1^0, of 3.8×10^{-4} cm/s, via (A24). By using this very simplified kinetic treatment of the h.e.r., the k_1^0 can be related to the exchange current density for this reaction, j_0, by the equation[18,19]

$$j_0 \approx Fk_1^0(C_{H^+})^{1/2}(C_{H_2})^{1/2} \quad (2)$$

where C_{H_2} is the solubility of H_2 at 1 atm, 7.7×10^{-7} mol/cm^3, α is taken as $^1/_2$, and the mechanism implied by eq A23 is assumed; with $C_{H^+} = 10^{-3}$ mol/cm^3 and the above value of k_1^0, log $j_0 \approx -3.0$ A/cm^2. The log j_0 values quoted for Pt for the h.e.r. generally range from −2.6 to −3.6.[19,20] Considering the assumptions and approximations made, this agreement is remarkable. A note of caution must be injected, however. The h.e.r. reaction is more complicated than the above treatment implies and the reaction mechanism may be different in acidic and alkaline solution and at different metals. Moreover, adsorption of organic compounds at electrode surfaces is known to affect the kinetics of the h.e.r.; both decreases (poisoning) and increases in the rate have been observed. Such adsorption will probably be a common occurrence in the types of systems employed in heterogeneous catalysis. Thus while the qualitative and semiquantitative trends are worth noting, calculation of absolute rates from tabulated electrochemical parameters is risky.

The variation of the H_2 evolution rate with catalyst material, as shown in Figures 2 and 4, also follows the model. Metals with smaller j_0 values (smaller k_1^0's) show lower values of $pH_{1/2}$. Because of the variation of j_0 values reported in the literature, as well as the problems alluded to above, a more quantitative treatment of these data is probably not justified.

Dependence on Mediator Potential. We have shown elsewhere that specific mediators of defined potential may be designed to shift the pH range for photocatalytic water reduction.[10] In the present model, changing the mediator corresponds to a shift of the anodic curve labeled med in Figure 1, along the potential axis. If the mediator potential, $E_{1/2}(\text{med})$, is more negative the anodic curve will shift until potential matching occurs at higher pH. If this potential is more positive, the potential match will occur at lower pH. In the region of potential matching ($pH_{1/2} \pm 1$ pH unit) a roughly linear dependence of rate on $E_{1/2}(\text{med})$ would be expected. Such behavior has indeed been observed; a linear plot of ($E_{\text{mediator}} - 0.059$ pH) vs. rate of (photocatalytic) H_2 production has been reported.[10] However, for pHs at which the rate is limited by mediator mass transport $pH < pH(i_l)$ one predicts that mediator potential would not affect the rate. This leveling effect

(18) A. J. Bard and L. R. Faulkner, "Electrochemical Methods", Wiley, New York, pp 100–101, 1980.
(19) J. O'M. Bockris, *Mod. Aspects Electrochem.*, **1**, 180–276 (1954).
(20) H. Kita and T. Kurisu, *J. Res. Inst. Catal., Hokkaido Univ.*, **21**, 200 (1973).

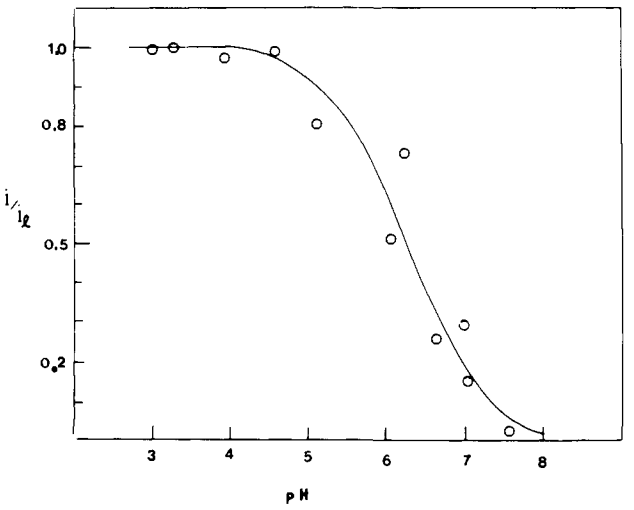

Figure 3. Theoretical and experimental correspondence of the electrochemical model for Pt catalysis. The solid line gives the predicted current i/i_{il} calculated numerically from eq A24 as a function of pH. $pH_{1/2}$ is taken from the photochemical data in Figure 2. The experimental points were obtained in an electrocatalytic experiment, using a methyl viologen mediator.

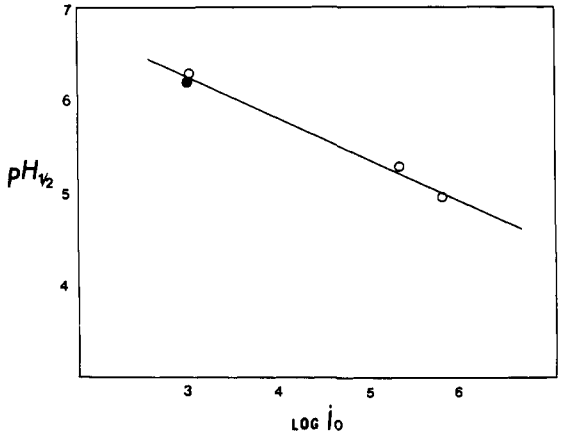

Figure 4. Dependence of the pH of half maximal rate, $pH_{1/2}$, on the exchange current density, i_0, for a series of different metals. The open points (O) were obtained in photocatalytic experiments. The closed point (●) was obtained in the electrocatalytic method.

is indeed observed in an electrogenerated mediator experiment. With the use of two mediators of different potential, $DMPB^{2+}$ ($E^0 = -0.6$ V) and MV^{2+} ($E^0 = -0.44$V), large differences in H_2 generation rate are observed at pH 7, but not at pH 3 where H_2 production is diffusion limited for both mediators. Analogous photocatalytic results have been reported by McLendon and Miller[10] and by Keller et al.[21] The latter authors found that $DMPB^{2+}$ produced H_2 more rapidly than MV^{2+} at pH <7, but, as predicted, no differences were observed at pH 5 for pH < pH(i_l).

Dependence on Colloid Composition. For any (large scale) application of metal colloid catalysts substitution of Pt by less expensive metals is clearly important. The present theory makes several predictions about such substitution. Any specific metal will have a characteristic rate constant or exchange current for hydrogen evolution.[19,20,22] In the present model the overpotential corresponding to a given current density will result in a shift of the water reduction waves along the potential axis. A higher hydrogen overpotential must be compensated by a lower pH to maintain an equivalent rate of H_2 generation. This expectation is confirmed by experiment. The present photocatalytic results show a clear correlation between the observed $pH_{1/2}$ for a metal

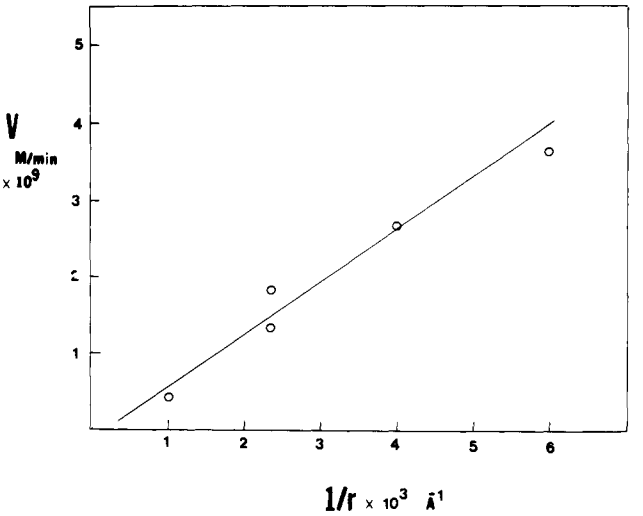

Figure 5. Dependence of the photocatalytic H_2 production rate (V) on colloid radius (r) for Au citrate colloids.

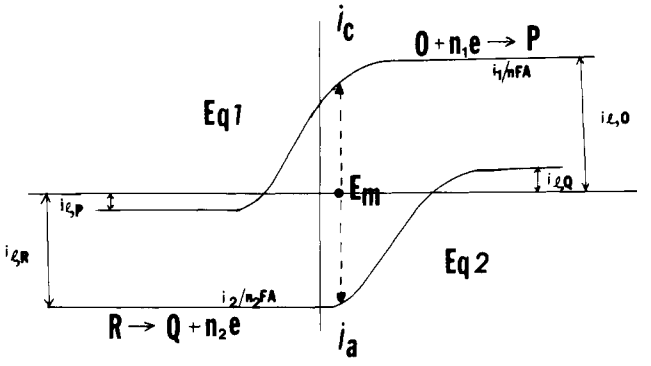

Figure 6. Schematic illustration of the electrochemical parameters used in the calculations.

colloid and the exchange current density, j_0, of that metal. The results of these experiments, plotted as $pH_{1/2}$ vs. log i_0, are shown in Figure 4.

The effect of colloid size may also be predicted by the electrochemical model. For spherical particles, for a given amount of catalyst, the surface area, A, will scale with size as the surface/volume ratio; A varies with 1/radius. Since the mass-transfer-limited current, i_l, is directly proportional to area, an inverse dependence of i_l on colloid radius would be expected at constant metal concentration.[23-26] Experiments with electrogenerated mediator and well-defined Au citrate colloids confirm this prediction. In Figure 5, the plot of i_l vs. $1/r$ shows the general linearity expected. Previously Gratzel et al. reported an elegant study of the effect of Pt colloid radius on H_2 yield in a photocatalytic system.[4] A replot of their data shows an excellent dependence of H_2 rate on $1/r_{Pt}$, as predicted.

In principle, it should be possible to calculate the absolute rate of hydrogen production at the mass transport limit, using the expression $i_l = FAm_RC_R$, where C_R is the concentration of reduced mediator, m_R the mediator mass transfer constant, and A the colloid surface area (see eq A9).[23] However, the colloid area cannot be readily determined, since the particles are not smooth spheres, but have a highly-convoluted, large-area surface. Moreover, the value of m_R is difficult to determine a priori under the usual convective conditions in such experiments. However, under given stirring conditions, m_R should be relatively constant

(21) P. Keller, A. Moradpour, E. Amouyal, and H. Kagan *J. Mol. Catal.*, 7, 539-542 (1980).
(22) J. O'M. Bockris and A. K. N. Reddy, "Modern Electrochemistry", Plenum Press, New York, Vol. 2, p 1238, 1970.
(23) Reference 18, p 28.
(24) Reference 18, p 96.
(25) H. B. Herman and A. J. Bard, *Anal. Chem.*, 35, 1121-1125 (1963).
(26) This simple linear dependence is only expected for a steady state experiment, where current is determined by convective mass transfer. For a potential step experiment a nonlinear platinum dependence might be expected.
(27) G. McLendon, to be published.

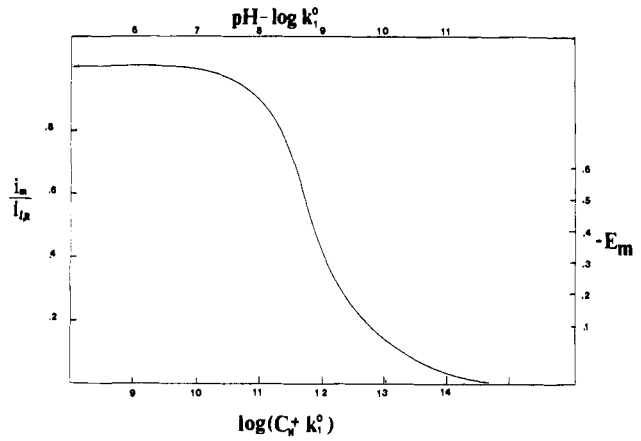

Figure 7. Sample plot of i/i_l vs. k_1, calculated from eq A24 for $[MV^{+\cdot}] = 10^{-2}$ M. The relationship between log k_1^0 and $pH_{1/2}$ can be obtained directly from such a plot.

and measurements of the limiting hydrogen evolution rate might be used to measure relative effective surface areas of colloidal particles. Experiments of this kind are proceeding.

Conclusions. The catalytic properties of the (colloidal) metal cocatalysts, which are widely used in current solar conversion schemes, can be understood and predicted by using a simple potential matching electrochemical model, similar to those used in corrosion and photocatalysis studies and those proposed by Spiro.[6,12] The present report provides both the quantitative theory and preliminary experimental verification to refine the currently popular "microelectrode" analogies for dispersed metal catalysts. Extensions of this approach should assist the rational design of catalytic systems for solar utilization.

Acknowledgment. G. McLendon gratefully acknowledges the support of an A. P. Sloan Fellowship and a Dreyfus Teacher-Scholar Award. D. Miller is an E. H. Hooker fellow. Work at Austin was supported by The National Science Foundation and the Welch Foundation.

Appendix I. Equations for Current-Potential Curves as Applied to Heterogeneous Catalysis.

A. General Equations. Consider the reaction of two soluble species, O and R, at the catalyst surface to form the soluble products P and Q in the overall reaction

$$n_2O + n_1R \xrightleftharpoons{\text{(catalyst)}} n_2P + n_1Q \qquad \text{(A1)}$$

This redox reaction occurs via the two half-reactions:

$$O + n_1e \rightleftharpoons P \qquad E_1^0 \qquad \text{(A2)}$$

$$Q + n_2e \rightleftharpoons R \qquad E_2^0 \qquad \text{(A3)}$$

We assume that no species is adsorbed or precipitated at the electrode surface and that the concentrations of the species at a given time, t, are C_O^*, C_R^*, C_P^*, and C_Q^*. Because these concentrations are changing with time, the reaction velocity, v (mol s^{-1} cm^{-2}), is also a function of time. We consider therefore an instantaneous velocity; a particularly convenient situation is at $t = 0$, where v is the initial velocity, v^0, determined when the products are absent (i.e., $C_P^* = C_Q^* = 0$).

The general i-E curves, shown in Figure 6, are governed by the equations:[19,24]

$$v_1 = \frac{i_1}{n_1FA} = k_1^0\{C_O(x=0)e^{-\alpha_1 z_1 f(E-E_1^0)} - C_P(x=0)e^{(1-\alpha_1)z_1 f(E-E_1^0)}\} \qquad \text{(A4)}$$

$$v_2 = \frac{i_2}{n_2FA} = k_2^0\{C_Q(x=0)e^{-\alpha_2 z_2 f(E-E_2^0)} - C_R(x=0)e^{(1-\alpha_2)z_2 f(E-E_2^0)}\} \qquad \text{(A5)}$$

where $C_j(x = 0)$ represents the concentration of the jth species at the catalyst surface, k_1^0 and k_2^0 are the standard rate constants for the heterogeneous electron transfer reactions (cm/s), and $f = F/RT = 38.96$ V^{-1}. The coefficients n_1 and n_2 represent the number of electrons exchanged in the overall half-reactions, while z_1 and z_2 represent the number exchanged in the rate-determining step (usually $z_1 = z_2 = 1$). The transfer coefficients, α_1 and α_2, are usually $\sim$0.5.

The concentration of O, P, ... at the particle surface ($x = 0$) can be expressed as functions of the bulk concentrations, C_O^*, C_P^*, ..., by considering the usual mass transfer limiting currents, $i_{l,O}$, $i_{l,P}$, ..., for the different species:[23]

$$i_{l,O} = n_1FAm_OC_O^* \qquad \text{(A6)}$$

$$i_{l,P} = -n_1FAm_PC_P^* \qquad \text{(A7)}$$

$$i_{l,Q} = n_2FAm_QC_Q^* \qquad \text{(A8)}$$

$$i_{l,R} = -n_2FAm_RC_R^* \qquad \text{(A9)}$$

where m_O, m_P, ... are the mass transfer coefficients (cm/s). The concentrations at the catalyst surfaces can be expressed in terms of these limiting currents as:

$$C_j(x=0) = \left(\frac{i_{l,j} - i_1}{i_{l,j}}\right)C_j^* \qquad j = O,P \qquad \text{(A10)}$$

$$C_j(x=0) = \left(\frac{i_{l,j} - i_2}{i_{l,j}}\right)C_j^* \qquad j = Q,R \qquad \text{(A11)}$$

We assume throughout that transport to the particle surfaces is a steady-state convective process, so that the mass-transfer coefficients would be functions of the diffusion coefficients, solution density and viscosity, stirring rate and mode, etc.[18] Under such conditions the actual geometric shape of the particles is not important. By combining (A4) with (A10) and (A5) with (A11) and solving for i_1 and i_2, the following general equations are obtained:

$$v_1 = \frac{i_1}{n_1FA} = \frac{C_O^* \exp(-\alpha_1x_1) - C_P^* \exp\{(1-\alpha_1)x_1\}}{\left[\frac{1}{k_1^0} + \frac{\exp(-\alpha_1x_1)}{m_O} + \frac{\exp\{(1-\alpha_1)x_1\}}{m_P}\right]} \qquad \text{(A12)}$$

$$v_2 = \frac{i_2}{n_2FA} = \frac{C_Q^* \exp(-\alpha_2x_2) - C_R^* \exp\{(1-\alpha_2)x_2\}}{\left[\frac{1}{k_2^0} + \frac{\exp(-\alpha_2x_2)}{m_Q} + \frac{\exp\{(1-\alpha_2)x_2\}}{m_R}\right]} \qquad \text{(A13)}$$

where $x_1 = z_1f(E - E_1^0)$ and $x_2 = z_2f(E - E_2^0)$. The general solution to the steady state rate of reaction A1 involves the condition

$$\frac{i_1}{n_1FA} = \frac{-i_2}{n_2FA} = v_m = \frac{i_m}{n_1n_2FA} \qquad \text{(A14)}$$

where v_m is the velocity of the mixed reaction and i_m is the mixed current, which occur at the mixed potential E_m. In principle, substitution of (A12) and (A13) into (A14) at $E = E_m$ should allow calculation of E_m, and use of this value in either (A12) or (A13) would yield i_m. However, closed form general solutions for E_m and i_m cannot be obtained. It is rather easy to write a digital computer program to locate the value of E_m which yields the condition in (A14) at various values of the electrode reaction parameters. Such a program, using the SOLVAR routine,[25] was written and values of E_m and i_m determined for different values of n_1, z_1, E_1^0, α_1, k_1^0, C_O^*, C_P^*, m_0, and m_P and the equivalent parameters for the Q, R reaction. The m values are determined from the limiting velocities, eq A6-A9.

B. Special Cases. Although (A12) and (A13) are general and hold for any value of the parameters, several limiting cases which

yield simpler equations are of interest and are given here for the sake of completeness.

i. **Nernstian Reactions; Initial Conditions.** When the heterogeneous electron-transfer reactions are very rapid ($k_1^0 \rightarrow \infty$; $k_2^0 \rightarrow \infty$) and $C_P^* = C_Q^* = 0$, the general equations yield:

$$i_1 = i_{l,O}/\{1 + \exp[n_1 f(E - E_{1/2,1})]\} \quad \text{(A15)}$$

$$i_2 = i_{l,R}/\{1 + \exp[-n_2 f(E - E_{1/2,2})]\} \quad \text{(A16)}$$

$$E_{1/2,1} = E_1^0 - \frac{1}{n_1 f} \ln \frac{m_O}{m_P} \quad \text{(A17)}$$

$$E_{1/2,2} = E_2^0 - \frac{1}{n_2 f} \ln \frac{m_Q}{m_R} \quad \text{(A18)}$$

ii. **Totally Irreversible Reactions.** When the rate of the back-reactions is negligible [$C_P^* \exp(1 - \alpha_1)x_1 \gg C_O^* \exp(-\alpha_1 x_1)$; $C_Q^* \exp(-\alpha_2 x_2) \gg C_R^* \exp(1 - \alpha_2)x_2$], then

$$\frac{i_1}{n_1 FA} = \frac{C_O^*}{\exp(a_1 x_1)/k_1^0 + 1/m_O} \quad \text{(A19)}$$

$$\frac{i_2}{n_2 FA} = \frac{-C_R^*}{\exp[-(1 - \alpha_2)x_2]/k_2^0 + 1/m_R} \quad \text{(A20)}$$

In the limit of no mass transfer effects ($m_O \rightarrow \infty$, $m_R \rightarrow \infty$), these yield the familiar Tafel-type equations

$$(i_1/n_1 FA) = k_1^0 C_O^* \exp(-\alpha_1 x_1) \quad \text{(A21)}$$

$$(i_2/n_2 FA) = -k_2^0 C_R^* \exp[(1 - \alpha_2)x_2] \quad \text{(A22)}$$

Expressions for the value of E_m and v_m for this limiting case, involving simultaneous solution of (A21) and (A22), have been previously given by Spiro.[12]

C. **Results for the Hydrogen Ion–Methyl Viologen Reaction.** The above treatment would apply to any electrode reaction by suitable modification of the general equations to account for adsorption, precipitation, etc. The hydrogen evolution reaction at metal electrodes has been the subject of numerous investigations.[19,20] While the form of the i–E expression depends upon the details of the electrode reaction mechanism, most mechanisms show a direct proportionality between i and C_{H^+}. For the calculations here we have employed the equation which applies under the conditions where the proton discharge step is rate determining and the steady state coverage by hydrogen atoms on the surface is small. Thus with $\alpha_1 z_1 = 0.5$ and $E_1^0 = 0.0$ V

$$i_1/FA = k_1^0 C_{H^+} \exp\{-0.5fE\} \quad \text{(A23)}$$

[equivalent to (A21)]. The reduction of methyl viologen is known to be rapid at Pt electrodes. Calculations for this couple were carried out by using general equation A13 with $m_Q = m_R = 10^{-3}$ cm/s, $z_2 = n_2 = 1$, $E_2^0 = -0.44$ V vs. NHE. For k_2^0 values of 10^{-2} cm/s or larger the results are independent of k_2^0, so that the reaction is essentially a nernstian reaction, eq A16. Because of the forms of A16 and A23, the results for the conditions where $E = E_m$ and (A14) applies can be given in terms of $i_m/i_{l,R}$ vs. log ($k^0 C_{H^+}$). Calculated values of these are shown in Figure 7. Note that a convenient reference point is where $(i_m/i_{l,R}) = 0.5$ and $E_m = E_{1/2}(2)$. This occurs at a particular pH, called $pH_{1/2}$; eq A24 is thus obtained.

$$pH_{1/2} = -\log \frac{i_m}{i_{l,R}} + \log (k_1^0) - \frac{\alpha_1 z_1 f E_{1/2}(2)}{2.3} - \log (m_R C_R^*) \quad \text{(A24)}$$

i.e.:

$$pH_{1/2} = 0.30 + \log k_1^0 - \left(\frac{\alpha_1 z_1 f E_m}{2.3}\right) - \log (m_R C_R^*)$$

Assuming the following conditions—$E_{1/2}$, $MV^{2+} = -0.44$ V; $\alpha_1 z_1 = 0.5$; $2.3/(\alpha_1 z_1 f) \simeq 0.12$ V; $m_R = 10^{-3}$ cm/s; and $C_R^* = 0.002$ M—gives

$$pH_{1/2} = \log k_1^0 + 9.73 \quad \text{(A25)}$$

Different values of C_R^* will therefore produce different $pH_{1/2}$ values.